INTERNATIONAL JOURNAL OF CURRENT RESEARCH IN CHEMISTRY AND PHARMACEUTICAL SCIENCES
(p-ISSN: 2348-5213: e-ISSN: 2348-5221)
www.ijcrcps.com
(A Peer Reviewed, Referred, Indexed and Open Access Journal)
DOI: 10.22192/ijcrcps Coden: IJCROO(USA) Volume 9, Issue 1 - 2022

Research Article

DOI: http://dx.doi.org/10.22192/ijcrcps.2022.09.01.003

Growth, spectral, thermal and mechanical studies on bisthiourea cobalt chloride single crystal: An efficient SHG material for NLO applications

T. Dhanabal*, B. Raja
Department of Chemistry, Muthayammal College of Engineering, Rasipuram, Namakkal-637408, Tamil Nadu, India.
*Corresponding author: E-mail: dhanabal27@gmail.com

Abstract

The title crystal was grown from saturated solution by slow evaporation solution growth technique at ambient temperature. The stoichiometric ratio of the crystal was confirmed by elemental analysis. The crystallinity of the crystal was confirmed by powder X-ray diffraction pattern. The UV cut-off wavelength is found to be at 250 nm it indicates the title crystal suitable for second harmonic generation. The thermal stability and decomposition pattern of the crystal were formulated by using TG-DTG and DTA studies. The FTIR spectroscopic technique was used to find out the various characteristic absorption bands present in the crystal. The SHG efficiency of the crystal indicates that the crystal has SHG efficiency twice than that of standard KDP. The mechanical properties of the crystal were measured by Vicker's microhardness test. The dielectric constant and dielectric loss of the crystals were decreases with increases in frequency.

Keywords: Crystal growth, Crystallization, Powder, X-ray diffraction, FTIR, Dielectric properties, SHG efficiency.

1. Introduction

Materials exhibiting large optical nonlinearity are of great interest for applications such as frequency conversion, telecommunication, optical computing, optical information processing and high optical disk data storage [1–3]. Organic materials show prominent properties due to their fast and large nonlinear response over a broad frequency range, inherent synthetic flexibility, and large optical damage threshold. However, organic materials may suffer from problems, such as volatility, low thermal stability, mechanical weakness, etc. Inorganic materials possess excellent mechanical and chemical properties but most of them show low nonlinear efficiency. The need for materials which combine large nonlinear optical characteristics with resistance to physical

and chemical attack has led to the investigation of semi-organics [4]. Under this circumstance, the quest for NLO materials is concentrated on a new class of materials called semiorganic crystals with high second harmonic generation (SHG) coefficients as well as stable physicochemical properties [5-8]. Due to their large nonlinearity, high resistance to laser induce damage, low angular sensitivity and good mechanical hardness, the semiorganic materials have the potentials for combing the high NLO property and chemical flexibility of organic materials with physical sturdiness and excellent transmittance of inorganic materials. Among the semiorganic NLO materials, metal-crystals of thiourea family have been investigated actively [9-11] and a variety of thiourea metal-crystal crystals have been grown [12-15]. Among the semi-organic materials, thiourea complex crystals are possessing good second harmonic generation (SHG) efficiency. The literature showed that the thiourea complex semiorganic crystals are exhibiting the nonlinear optical properties and the several researchers have been reported on thiourea complexes such as bis(thiourea) cadmium formate (BTCF), bis(thiourea) cadmium acetate (BTCA), zinc tris(thiourea) sulphate (ZTS), bis(thiourea) cadmium chloride (BTCC) [16], bis(thiourea) zinc chloride (BTZC), tris (thiourea) cadmium sulphate (TTCS), potassium thiourea bromide (PTB) and tri(thiourea) silver (I) nitrate (TTSN). Thiourea molecules are an interesting in organic matrix modifier due to its large dipole moment and its ability to form and extensive network of hydrogen bonds. The centrosymmetric thiourea molecule, when combined with inorganic salt yield non-centrosymmetric complex, which has the nonlinear optical properties. Motivated by the intriguing properties of this material, an attempt has been made to synthesize and growth of thiourea crystal. These grown crystals were subjected to C H N S, powder XRD, UV transmittance, TG-DTA, FTIR, NLO, microhardness and dielectric studies and the results obtained are reported here and discussed.

2. Experimental details

2.1. Growth of single crystals of BTCC crystal

Single crystals of bisthiourea cobalt chloride (abbreviated as BTCC) were grown by slow evaporation of saturated aqueous solutions at room temperature. Two moles of thiourea and one mole of cobalt chloride react to form BTCC crystals. Aqueous solutions containing analytical grades of thiourea and cobalt chloride in 2:1 molar ratio respectively was prepared by using triply distilled water. The two solutions were mixed together and stirred well for about 4 h and then resulting solution was filtered through a Whatmann 42 filter paper into a clean dry beaker. The beaker was covered by an ordinary filter paper. Care was taken to minimize the temperature gradient and mechanical shock. The formation of BTCC according to the following equation.

$$2(NH_2CSNH_2) + CoCl_2 \rightarrow \underset{\text{BTCC}}{(NH_2CSNH_2)\,CoCl_2}$$

Bright, transparent and yellow coloured BTCC crystals were obtained. Crystallization took place within 15 to 20 days. The grown crystals were collected from the mother liquid by using well cleaned forceps. The harvested crystals were recrystallized repeatedly to get crystals of good quality.

2.2. Characterization of BTCC crystal

C H N S analysis of BTCC crystal was carried out using ELEMENTAL VARIO EL III MODEL analyzer, (STIC) Cochin. The powder XRD patterns of BTCC crystal were obtained using BRUKER AXS D8 Advance X-ray diffractometer model instrument with Cu Kα radiation (λ = 1.54060 Å) at room temperature. The UV-VIS-NIR a study of BTCC was carried out by using JASBO V-550 spectrometer. The thermal analysis (TG and DTA) of BTCC were recorded using a

PERKIN ELMER DIAMOND thermal analyzer under nitrogen atmosphere. The FTIR spectra of BTCC crystal were recorded using a Perkin Elmer model RX1 instrument. The second harmonic generation efficiency of the crystal was carried out by modified Kurtz-Perry powder technique using Nd:YAG laser. The mechanical properties of the crystal were measured using Vicker's microhardness test. The dielectric properties of the crystal were studied at room temperature using a TH 2816 A DIGITAL LCRZ METER in the frequency region from 50 Hz to 5 MHz.

3. Results and Discussion

3.1. Elemental analysis

The elemental analysis data obtained for BTCC crystals given in Table 1**.** It is evident that the experimental and calculated percentages of Carbon, Hydrogen, Nitrogen and Sulphur are very close to each other and are within the experimental errors. The elemental analysis data of the crystal confirms the formation of the crystal in the stoichiometric proportion**.** The calculated elemental percentages of C, H, N and S were obtained by using the molecular formula $C_2H_8N_4S_2CoCl_2$ of the expected crystal. Thus, the stoichiometric ratio of the crystal was confirmed.

Table 1. Elemental analysis of BTCC crystal.

Element	C%	H%	N%	S%
Experimental	8.75	2.86	16.19	23.56
Calculated	8.88	2.96	16..29	23.70

3.2. Powder X-ray diffraction method

The powder X-ray diffraction pattern of BTCC is shown in Figure 1. The sharp and well-defined Bragg peak at specific 2θ value in the powder XRD pattern confirms its crystallinity. The 2θ values observed in the powder X-ray diffraction pattern were used to calculate the lattice parameters and unit cell volume by using the CRYSFIRE software package The unit cell parameters obtained are a = 17.5210Å, b = 12.6242Å,c = 13.8541Å and α = γ = 90°, β ≠ 90° and the unit cell volume is 2213.1Å^3. From the unit cell parameters, it is observed that the crystal crystallizes in monoclinic system.

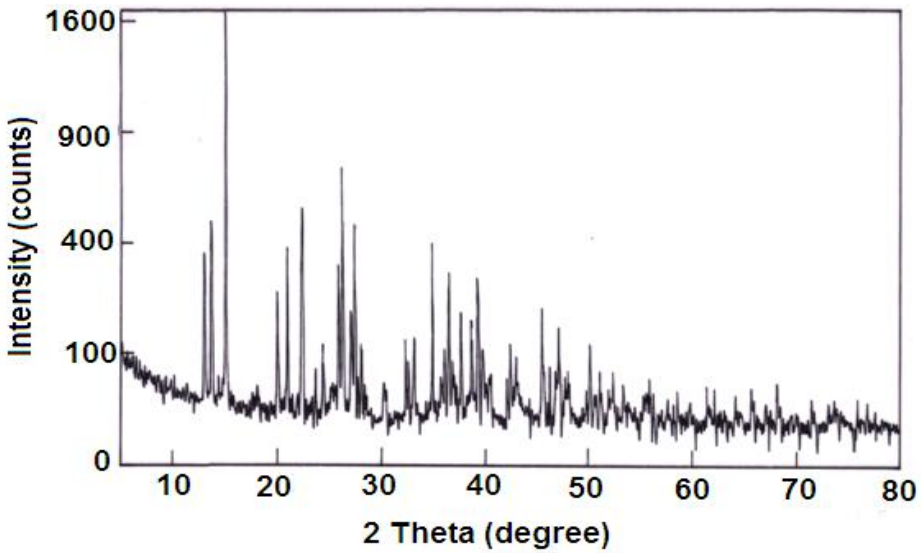

Figure 1. Powder XRD pattern of BTCC crystal.

3.3. UV-visible transmittance spectral analysis

The UV-visible transmittance spectrum of the crystal is shown in Figure 2. From the graph, it is observed that the crystal shows a cut-off wavelength at 360 nm. The lower cut-off wavelength at 360 nm is due to the n-π* transition of the constituent groups. There is no absorption observed between 360 and 900 nm in the entire visible region. Hence, the material may be useful for optoelectronic application in the region from 360 to 900 nm. The crystal has 75% transparency. The higher intensity of absorption band present in the UV region is due to the conjugated systems present in the grown material.

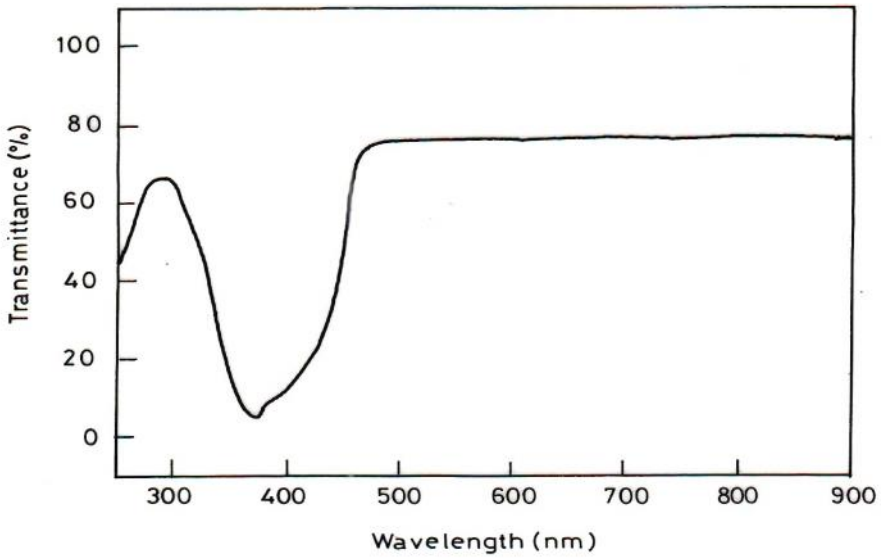

Figure 2. UV-visible transmittance spectrum of BTCC crystal.

3.4. Thermal analyses

3.4.1. Thermogravimetric analysis

The TG-DTG thermograms of the crystal BTCC are shown in Figure 3. The crystal was subjected to uniform heating at a heating rate of 10°C per minute at nitrogen atmosphere. The crystal BTCC decomposes in single stage when it is heated from room temperature to 1200°C. The crystal is found to be stable up to 150°C. Afterwards, it decomposes in a single stage between 170 and 800°C. It is evident that the crystal decomposes on heating up to about 800°C. During this portion of heating the entire molecule is decomposed leaving behind the metal, cobalt. The experimental weight loss for this portion is 88%. The calculated weight loss is 87%. The close agreement between the experimental and calculated weight losses confirms the formation of the compound. The thermal derivative curve in DTG (solid curve) study conforms to the weight loss pattern in the TG curve. Thus the DTG study confirms the weight losses observed in the TG thermograms.

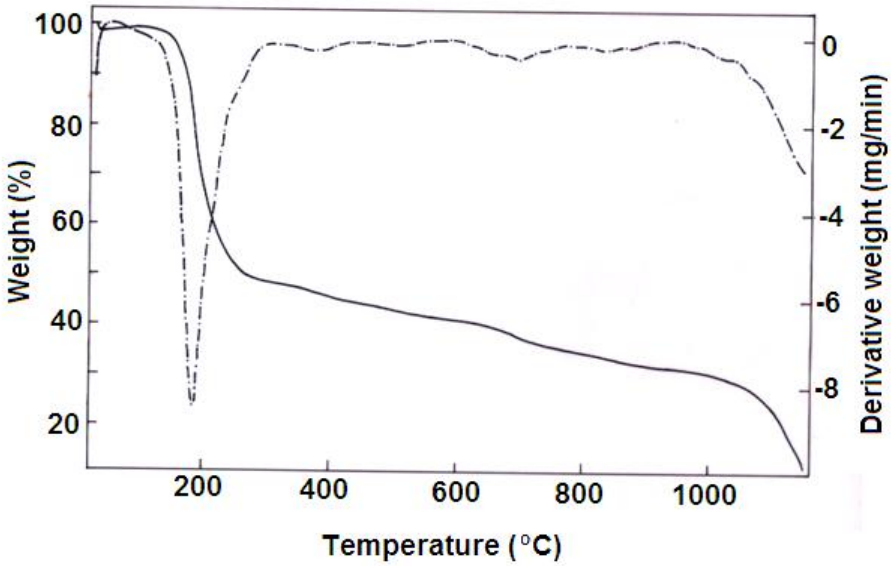

Figure 3. TG-DTG thermogram of BTCC crystal.

3.4.2. Differential thermal analysis

The DTA curve of the crystal BTCC is shown in Figure 4. Two endothermic peaks are observed. The endothermic peaks appear between 170 and 700°C is due to the entire molecule is decomposed leaving behind the metal, cobalt.

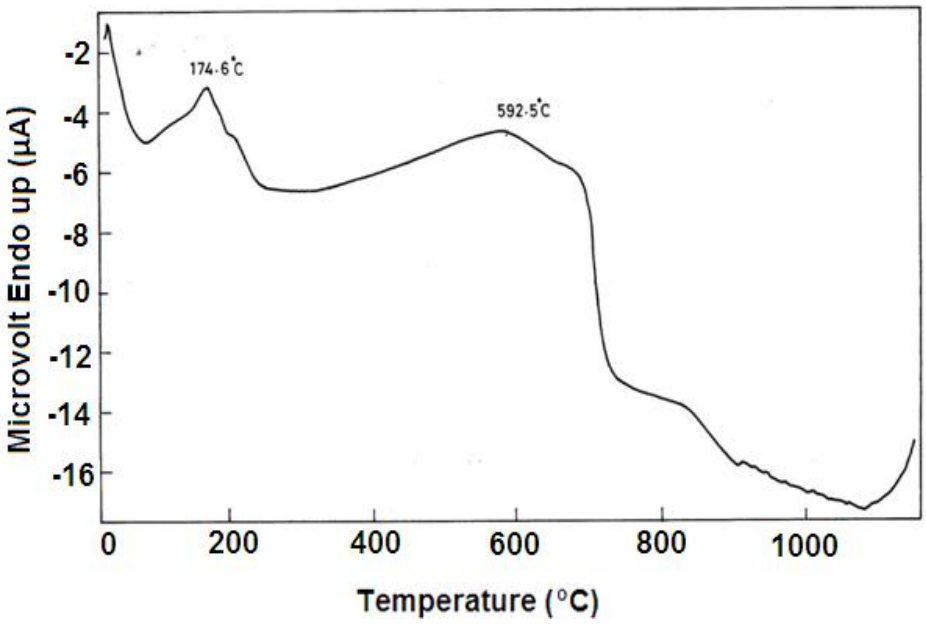

Figure 4. DTA thermogram of BTCC crystal.

3.5. FTIR spectral analysis

The FTIR spectrum of BTCC is shown in Figure 5. The NH_2 stretching vibration is observed at 3285 cm^{-1}. The absorption at 3193 cm^{-1} is assigned to N-H stretching vibration. The C-H stretching vibration is observed at 2751 cm^{-1}. The absorption at 2381 cm^{-1} is characteristic of C-C bond stretching vibration. The combination band and overtone for appear at 2184cm^{-1}.

The NH_2 bending vibration observed at 1880cm$^{-1.}$ The peak at 1632 cm^{-1} is assign to N-H bending vibration. The absorption at 1414 cm^{-1} is due to presence of C-N stretching vibration. The N-H rocking vibration is observed at 1106 cm^{-1}. The peak absorbed at 663 cm^{-1} and 448 cm^{-1} are due to metal chloride, Co-Cl stretching vibrations.

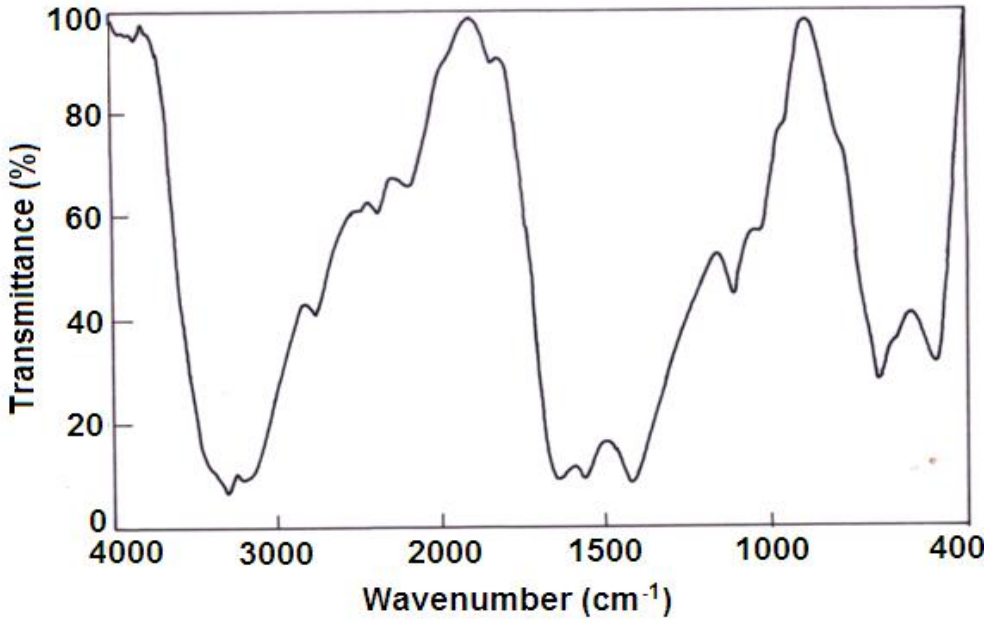

Figure 5. FTIR spectrum of BTCC crystal.

3.6. Non-linear optical study

The nonlinear property of the sample was determined by the modified version of the Kurtz and Perry [17] powder technique using a Nd:YAG laser with a pulse repetition rate of 10 Hz working at 1064 nm. The sample was ground into fine powder and it is tightly packed in a micro-capillary tube. It was mounted in the path of the laser beam of 3.1 mJ pulse energy obtained by splitting the original laser beam. The output light was passed through a monochromator transmitting only the second harmonic (green) light at 532 nm. The green light intensity was registered by a photomultiplier tube and converted into an electrical signal. This signal was displayed on the oscilloscope screen. Second Harmonic Generation (SHG) conversion efficiency was computed by the ratio of signal amplitude of the sample to that of the Potassium dihydrogen phosphate (KDP) signal amplitude recorded for the same input powder. The emission of green light from the title sample indicates that the sample shows the second harmonic generation efficiency. The SHG efficiency of the crystal may be due to the presence of intermolecular hydrogen bonding in the crystal lattice and also the presence remarkable hyperpolarizability of the title crystal.

3.7. Microhardness measurement

Hardness is an elegant property to characterize a material and it is a measure of the resistance to deformation, which is directly related to the forces that exist between atoms in solids. For microhardness measurement, the crystal surface was carefully lapped and polished to avoid surface effects which influence the hardness value strongly. The selected surface of the crystal was polished using a velvet cloth to get a smooth surface.

The indentation time of the crystal was fixed as 10 s for each trial. Loads of 25, 50 and 100 g were used to analyze the microhardness studies. The variation of hardness value with applied load is shown in Figure 6.

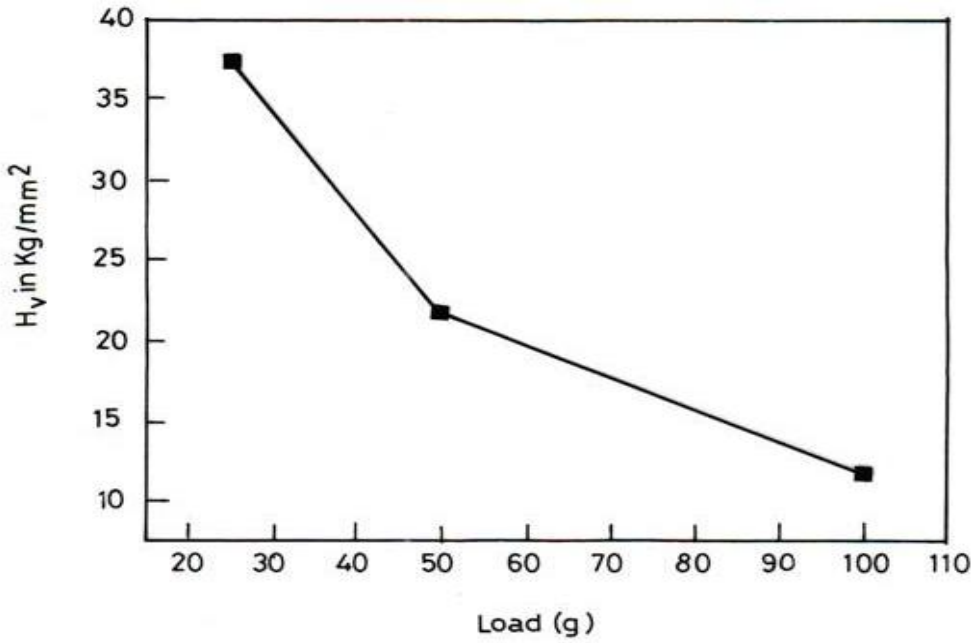

Figure 6. Variation of hardness with applied load BTCC crystal.

From the plot, it is seen that the hardness value of the material decreases with increase of loads up to 50 mg and above 50 g, the crack starts on the crystal which is evident slight downward deviation from the line. A decreasing trend is observed in the hardness values with increasing applied load and hence the indentation size effect (ISE) is satisfied. The hardness values of the material was calculated using following relation,

$$H_v = 1.8544\ P/d^2\ (kg/mm^2)$$

A plot between log 'd' and log 'P' is shown in Figure 7, which gives a straight line. The Mayer's law is, $P = ad^n$, where 'n' is the work hardening coefficient and 'a' is the constant. The value of work hardening co-efficient, n was calculated from the slope of the straight line. The value of work hardening co-efficient of the crystal was found to be 1.8. The value of n for this crystal indicates that BTCC is a soft material.

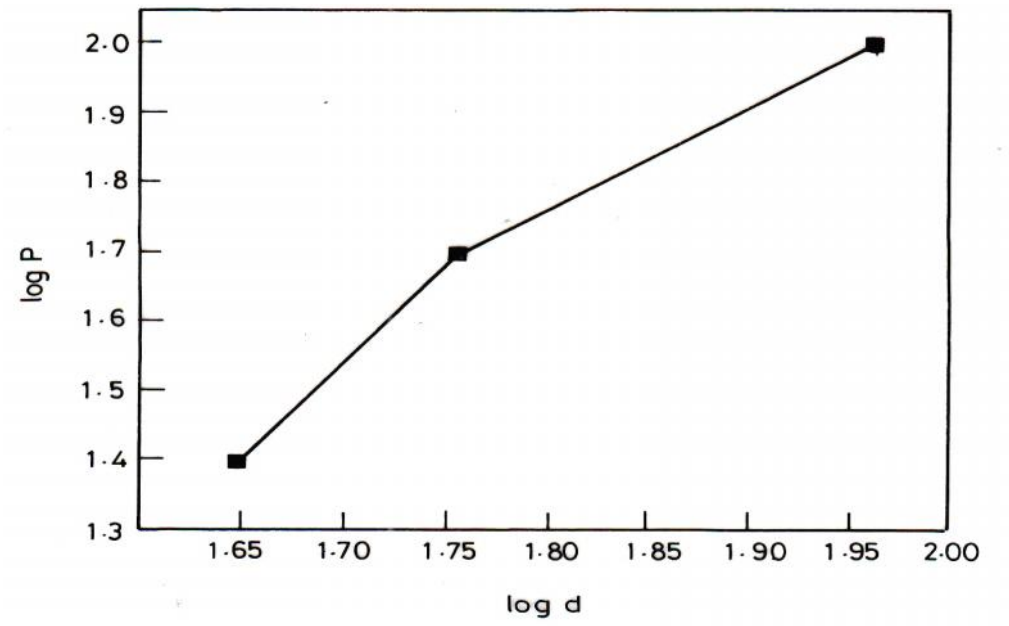

Figure 7. Plot of log d versus log P of BTCC crystal.

3.8. Dielectric studies

Good quality of single crystal of as BTCC was selected for the dielectric measurements using LCR meter in the frequency from 50 Hz to 5 MHz. The sample was polished by soft tissue paper. Silver paste was applied on both opposite faces to make a capacitor with the crystal as a dielectric medium. The sample was placed between two cooper electrodes, which acts as a parallel plate capacitor. The capacitance and dielectric loss were measured for different frequencies from 50 Hz to 5 MHz. The dielectric constant was calculated using the following relation

$$\varepsilon_r = Ct/\varepsilon oA$$

where C is the capacitance, d is the thickness of the crystal, εo is the vacuum dielectric constant and A is the area of the crystal. The variation of dielectric constant with log υ is depicted in Figure 8. From the graph, it is observed that the dielectric constant decreases with increase in frequency. This effect can be attributed to the effect of charge distribution by mass carrier hopping on defects. The values of dielectric constants are high at lower frequencies and they are low at higher frequency region. The large values of dielectric constant at lower frequencies suggest that there is a contribution from all the fours known sources of polarizations namely, electronic, ionic, dipolar and space charge polarizations. Space charge polarization is generally active at lower frequencies. The space charge polarization will depend on the purity and low perfection of the material.

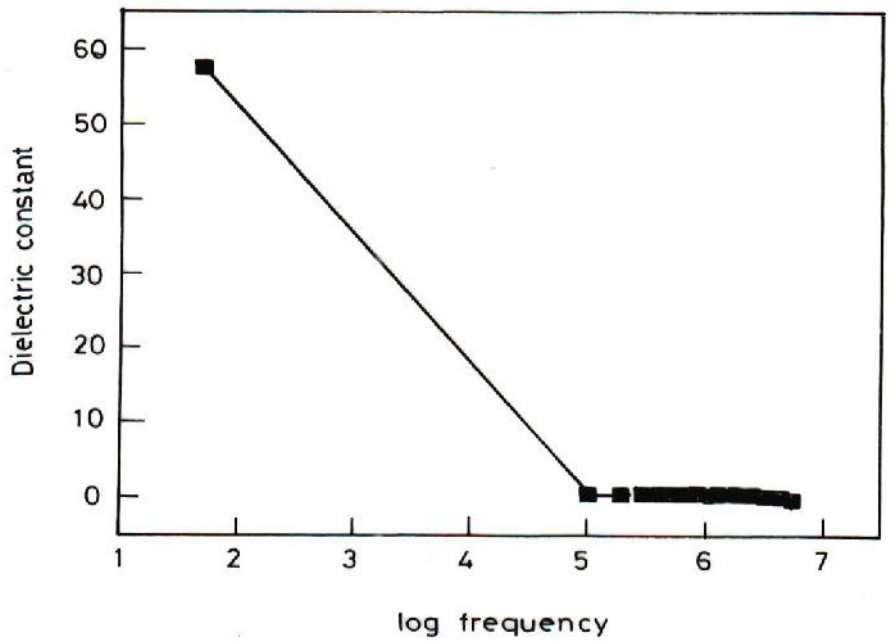

Figure 8. Variation of dielectric constant with log frequency.

The variation of dielectric loss with log υ is shown in Figure 9. From the plot, it is observed that the dielectric loss decreases with increase in frequencies. The values of dielectric loss are high at lower frequencies and are low at higher frequency region. The low values of dielectric loss suggest that the sample possesses enhanced optical quality with lesser defects and this parameter is of vital importance for optoelectronic applications.

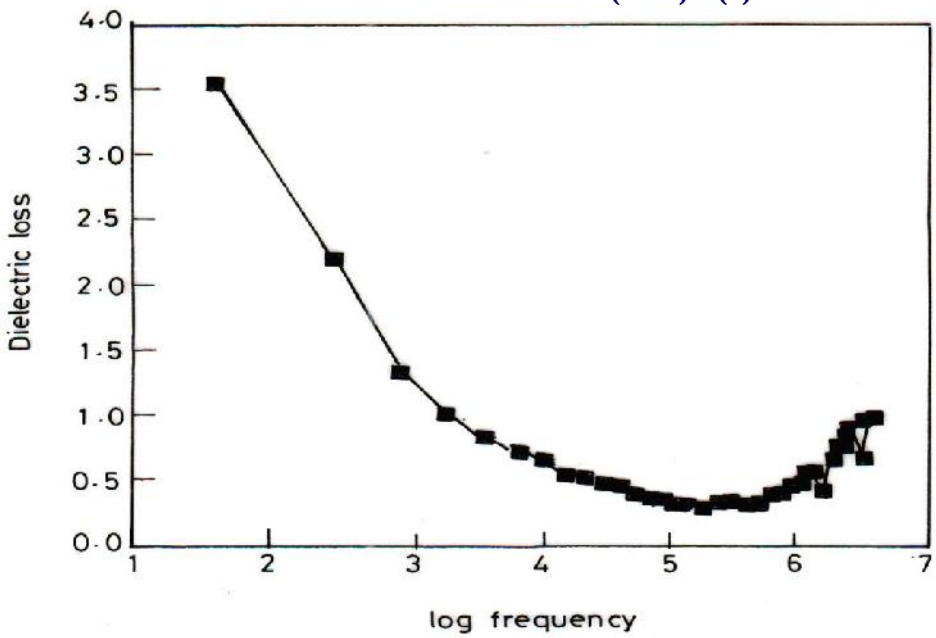

Figure 9. Variation of dielectric loss with log frequency.

4. Conclusions

Single crystal of bisthiourea cobalt chloride was grown from saturated solution by slow evaporation solution method. The elemental analysis data of crystal confirms stoichiometric ratio of the crystal. The powder XRD of the crystal confirms the crystallinity of the crystal. The optical property of the crystal was confirmed by UV-visible absorption study. The thermal stability and decomposition pattern of the crystal were formulated by using TG-DTA studies. The FTIR spectroscopic technique was used to find out the various characteristic absorption bands present in the crystal. The SHG efficiency of the crystal was confirmed by Kurtz-Perry powder technique. The mechanical properties of the crystal were measured using Vicker's microhardness test. The dielectric constant and dielectric loss of the crystals were decreases with increases in frequency.

Acknowledgments

The authors T. Dhanabal and B.Raja gratefully acknowledge the Chairman, Secretary of Muthayammal College of Engineering, Rasipuram, Tamil Nadu, India for their constant encouragement and support. The author T.Dhanabal also acknowledges the School of Chemistry, University of Hyderabad for their instrumental facilities.

References

[1] I.Ledoux , Synth. Met. 54 (1993) 123.
[2] D.R. Yuan, D. Xu, N. Zhang, M.G. Liu, M.H. Jiang Chin. Phys. Lett. 13 (1996) 841.
[3] M. Iwai, T. Kobayashi, H. Furya , Y. Mori, T. Sasaki, Jpn. J. Appl. Phys. 36 (1997) 276.
[4] A. Arunkumar, P. Ramasamy, Mat. Lett. 123 (2004) 246.
[5] N. Zhang, M. Jiang, D. Yuan, D. Xu, X. Tao, Chin. Phys. Lett. 6 (1989) 289.
[6] S. Selvakumar, S.A. Rajasekar, K. Thamizharasan, S. Sivanesan, A. Raman, P. Sagayaraj, Mater. Chem. Phys. 93 (2005) 356.
[7] N.P. Rajesh, V. Kannan, M. Ashok , M. Sivaji, J. Cryst. Growth, 262 (2004) 561.
[8] M.L. Caroline, S. Vasudevan, Mater. Chem. Phys. 113 (2009) 670.
[9] L.F. Warre, R.E. Allred, R.J. Martinez, W.B. Wischmann, "Proceedings of the Fourth International SAMPE Electronics Conference", 4 (1990) 388.
[10] W.B. Hou, D. Xu, D.R. Yuan, M.G. Liu, Cryst. Res. Technol. 29 (1994) 939.

[11] J.M. Alia, H.G.M. Edwards, M.D. Stoev, Spectrochim. Acta. Part A, 55 (1999) 2423.
[12] H.O. *Marcy, L.F. Warren, M.S. Webb,* C.A. Ebbers, S.P. Velsko, G.C. Kennedy, G.C. Catella, *Appl. Opt. 31 (1992) 5051.*
[13] P.M. Ushashree, R. Muralidharan, R. Jayavel, P. Ramasamy, J. Cryst. Growth, 21 (2000) 3651.
[14] D. Jayalakshmi, R. Sankar, R. Jayavel, J. Kumar, J. Cryst. Growth, 276 (2005) 243.
[15] K. Selvaraju, R. Valluvan, S. Kumararaman, Mater. Lett. 61(2007) 751.
[16] M. Lawrence, J. Thomas Joseph Prakash, Spectrochim. Acta Part A, 91 (2012) 30.
[17] S.K. Kurtz, T.T. Perry, J. Appl. Phys. 39 (1968) 3798.

Access this Article in Online

Website: www.ijcrcps.com

Subject: Chemistry

Quick Response Code

DOI: 10.22192/ijcrcps.2022.09.01.003

How to cite this article:
T. Dhanabal, B. Raja. (2022). Growth, spectral, thermal and mechanical studies on bisthiourea cobalt chloride single crystal: An efficient SHG material for NLO applications. Int. J. Curr. Res. Chem. Pharm. Sci. 9(1): 14-23.
DOI: http://dx.doi.org/10.22192/ijcrcps.2022.09.01.003

